Standing Calcium Gradients in Olfactory Receptor Neurons Can Be Abolished by Amiloride or Ruthenium Red

FRITZ WALTER LISCHKA and DETLEV SCHILD

Physiologisches Institut, Universität Göttingen, Humboldtallee 23, D-37070 Göttingen, Germany

ABSTRACT Digital imaging and the patch clamp technique were used to investigate the intracellular calcium concentration in olfactory receptor neurons using the Ca^{2+} indicator dyes fura-2 and fura-2/AM. The spatial distribution of Ca_i^{2+} as well as its modification by the drugs Amiloride and Ruthenium Red were studied.

Resting calcium concentrations in cells loaded with fura-2/AM were between 10 and 200 nM. In cells that were loaded with the pentapotassium salt of fura-2 through the patch pipette, calcium concentrations were in the same range if ATP was added to the pipette solution. Otherwise, Ca^{2+} reached concentrations of ~500 nM.

Most of the observed cells showed a standing gradient of calcium, the calcium concentrations in the distal dendritic end of the cell being higher than in the soma. In some cells, the gradient was markedly reduced or abolished by adding either Amiloride or Ruthenium Red to the bath solution. In a few cells, neither drug had any effect upon the gradient.

It is suggested that the inhomogenous spatial distribution of intracellular calcium in olfactory cells of *Xenopus laevis* is brought about by an influx of calcium ions through two different calcium permeable conductances in the peripheral compartments of the cells. The fact that only either Ruthenium Red or Amiloride abolished the standing calcium gradient further suggested that the two conductances blocked were presumably not coexpressed in the same cells.

INTRODUCTION

Over the last years, considerable understanding of olfactory transduction processes has been gained. Odor molecules appear to interact with membrane bound receptor proteins of olfactory receptor neurons, and activation of the cells occurs through second messenger pathways. The best established pathway involves cAMP as a second messenger, and the cascade elements of this pathway well known from other systems have now been described in olfactory neurons (Pace, Hanski, Salomon, and Lancet, 1985; Sklar, Anholt, and Snyder, 1986; Nakamura and Gold, 1987; Jones and Reed,

Please address correspondence to Dr. D. Schild, Physiologisches Institut, Universität Göttingen, Humboldtallee 23, D-37073 Göttingen, Germany.

J. GEN. PHYSIOL. © The Rockefeller University Press · 0022-1295/93/11/0817/15 $2.00
Volume 102 November 1993 817–831

1989; Dhallan, Yau, Schrader, and Reed, 1990; Boekhoff, Tareilus, Strotmann, and Breer, 1990; Breer, Boekhoff, and Tareilus, 1990; Buck and Axel, 1991). In amphibia, odor activated currents have been reported in isolated olfactory cells of the salamander, the frog, the clawed frog, the tiger salamander, the newt, and the mudpuppy (Trotier, 1986; Frings and Lindemann, 1988; Firestein and Werblin, 1989; Kurahashi, 1989, 1990; Kurahashi and Shibuya, 1989; Firestein, Shepherd, and Werblin, 1990; Dionne, 1992; Lischka and Schild, 1993). The odor activated and cAMP-gated conductance appears to be permeable for cations including Ca^{2+} (Kurahashi and Shibuya, 1990). In addition, it seems to be blocked by Ca^{2+} (Kurahashi, 1989; Zufall, Shepherd, and Firestein, 1991) and to decrease its sensitivity to cAMP with increasing intracellular concentrations of calcium (Lynch and Lindemann, 1992). This conductance is blocked by Amiloride (Frings, Lynch, and Lindemann, 1992).

In other vertebrate species including man, a different olfactory second messenger pathway via IP_3 and Ca^{2+} has been reported (Restrepo, Miyamoto, Bryant, and Teeter, 1990; Restrepo and Boyle, 1991). Activation of olfactory neurons through this pathway has been shown to be blocked by Ruthenium Red (Restrepo et al., 1990).

Furthermore, calcium is reported to be involved in several other membrane processes in olfactory cells; first, a voltage-activated Ca^{2+} conductance as well as a calcium-dependent potassium conductance have been described (Trotier, 1986; Firestein and Werblin, 1987; Schild, 1989; Restrepo and Teeter, 1990). Second, there is a ciliary, Ca^{2+}-activated chloride conductance (Kleene and Gesteland, 1991) as well as a Ca^{2+}-activated cation conductance (Schild and Bischofberger, 1991). Their precise physiological role remains to be investigated in more detail.

Given this multiple involvement of calcium in olfactory cells, it seemed intriguing to measure the intracellular calcium concentrations directly. We have found that the calcium concentration in most olfactory cells of *Xenopus laevis* shows a standing gradient which is abolished either by Amiloride or by Ruthenium Red. To account for a possible influence of the patch clamp whole-cell configuration upon the intracellular calcium concentration, we measured Ca_i^{2+} in isolated receptor cells under whole-cell recording conditions as well as in non-patch-clamped receptor cells.

MATERIALS AND METHODS

Preparation and Tissue Dissociation

The procedures were very similar to those described previously (Schild, 1989). Briefly, adult *Xenopus laevis* were purchased from a commercial source (Kähler, Hamburg, FRG) and held in aquaria at room temperature. The animals were decapitated after anaesthesia in a mixture of water and ice. Skin, cartilage, and bone above the olfactory organ were removed. The mucosa of the main olfactory cavity was separated from the underlying tissue; the caudal olfactory nerve twigs were transsected, and the mucosae were extirpated and put into the dissociation solution (see below). Enzymes were not applied in order to prevent alterations of membrane proteins involved in the transduction process. The mucosae were then mechanically disrupted in a drop of dissociation solution (~ 100 μl), triturated with a plastic pipette (2 mm i.d.), and then 100 μl of Ringer solution was added to the cell suspension. The cells were stored at 5°C and used within 6 h. 50 μl of the cell suspension was put onto a glass coverslip within the experimental

chamber (vol 100 μl). Coverslips were coated with Concanavalin A (0.3 mg/ml). Only cells which had retained their cilia during the dissociation procedure were used.

Cell Loading with fura-2

Two alternative ways of loading olfactory cells with fura-2 were used; the dye either entered the cells in its ester form across the plasma membrane or it diffused from the patch pipette into the cell.

As soon as the cell suspension was prepared, aliquots of 50 μl were distributed onto the experimental chambers. Cells were stored at 4°C. 30 min before recording, 50 μl of a Ringer solution containing 100 μM fura-2-acetoxymethylester(AM) was added to the charge. The solution containing 100 μM fura-2/AM was prepared as follows: 50 μg Fura/AM (Molecular Probes, Inc., Eugene, OR) were dissolved in 5 μl dry DMSO (Sigma Chemical Co., St. Louis, MO) and added to 445 μl Ringer (R5) and 50 μl pluronic acid (2,5%) (Pluronic F127, Molecular Probes, Inc.).

Alternatively, cells studied in the whole-cell configuration were loaded with the pentapotassium salt of fura-2 (Molecular Probes, Inc.) through the patch pipette. The final fura-2 concentration in the pipette was 0.2 mM.

The pixel values of fluorescence images taken from ester-loaded cells were in the same range or lower than in corresponding images taken from cells that were loaded with fura-2 through the pipette. Presumably, the net uptake of fura-2/AM was slow. We had no evidence for incomplete deesterification.

Patch Clamp Whole-Cell Configuration

All patch clamp experiments were done in the whole-cell configuration (Hamill, Marty, Neher, Sakmannn, and Sigworth, 1981) and the procedures were identical to those reported previously (Schild and Bischofberger, 1991). Electrodes of 7 MΩ resistance were fabricated from borosilicate glass (1.8 o.d., Hilgenberg, Malsfeld, FRG) using a custom-made two stage electrode puller.

The patch clamp setup, consisting of the amplifier (EPC7, List, Darmstadt, Germany), data recording with PCM unit (Instrutech VR100), video recorder, and a computer (VME/Eurocom5, ELTEK, Darmstadt, Germany) is shown in Fig. 1. The voltage clamp pulse protocol program was written in "C" and ran on a secondary processor board (SAC7, ELTEK) the VME computer, which delivered the command signals to a 12 bit D/A converter. The resulting pulses were fed to the patch clamp amplifier. Seal resistances were in the range of 3 and 20 GΩ. Whole-cell break-through was achieved by brief suction pulses or by short negative voltage pulses. The cells were voltage clamped at a potential of −80 mV throughout the experiments.

Solutions

The following solutions were used (concentrations in mM): dissociation solution: NaCl 106, KCl 2.5, Hepes 1; pH = 7.8, 215 mosm; Ringer (R5): NaCl 106, KCl 4, $CaCl_2$ 5, $MgCl_2$ 0.5, Glucose 1, Hepes 1; pH = 7.8, 230 mosm; pipette solution: NaCl 20, KCl 65, $MgCl_2$ 5, EGTA 3, ATP 1, fura-2 0.2, Hepes 10; pH = 7.8, 180 mosm.

In some experiments ATP was omitted from the pipette solution and isosmotically replaced by KCl. The bath solutions R0.02 and R1 were identical to the solution R5 except that the calcium concentrations were 0.02 and 1 mM, respectively, with appropriately adjusted concentrations of NaCl for isosmolarity. In some experiments, Amiloride or Ruthenium Red were added to the bath solution at final concentrations of 50 and 10 μM, respectively.

CCD-Camera Imaging and Measurement of Intracellular Calcium

A sketch of the patch-clamp and imaging setup is shown in Fig. 1. A 150 W Xenon arc lamp (Amko, Tornesch, Germany) was used for exciting the Ca-indicator dye fura-2 at 340 nm and 380 nm. The light passed an infrared filter (quarz windows, water, 7 cm pathlength) and was coupled through a UV-light guide to a filterwheel (Luigs & Neumann, Ratingen, Germany), which was mounted to an inverted microscope (Zeiss, Axiovert 35). We equipped the filterwheel with interference filters at 340 and 380 nm (Lys&Optik, Lyngby, Denmark), and mounted a

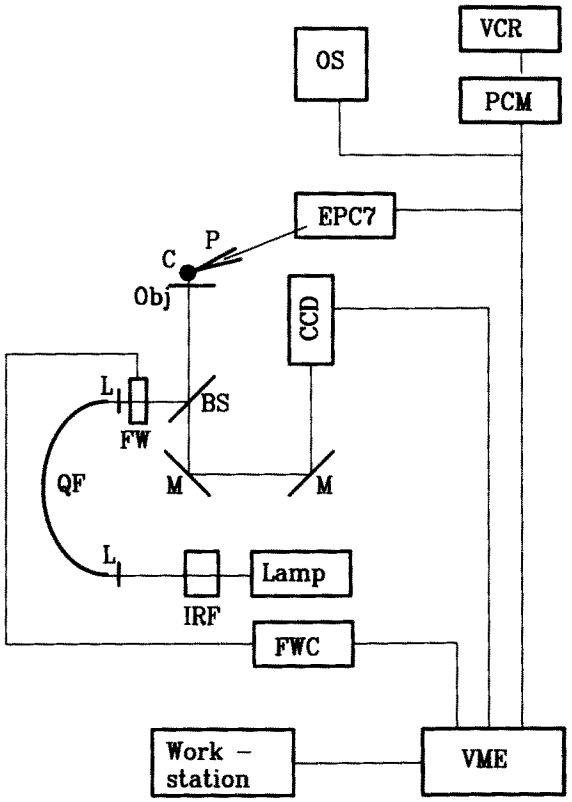

FIGURE 1. Sketch of the experimental setup for patch clamp and optical recording. An olfactory cell (*C*) is sealed on a patch pipette (*P*). The amplified pipette signals are sent from the patch clamp amplifier (*EPC7*) to an oscilliscope (*OS*) and to a pulse code modulation unit (*PCM*) with video recorder (*VCR*). The command voltage is delivered from the com puter (*VME*) and a digital-to-analog converter (not shown). Epifluorescence illumination is done by a 150 W Xenon arc lamp (*Lamp*), infrared water filter (*IRF*), focusing lenses (*L*), and a UV light wave guide (*QF*). The excitation wavelengths (340 or 380 nm) are determined by the position of a filterwheel (*FW*) which is controlled by a hardware controller unit (*FWC*) and the VME computer. The excitation light is then reflected by the beam splitter (*BS*) and directed onto the cell (*C*) through an 63× Zeiss objective. Fluorescence images pass the beam splitter and are deflected by mirrors (*M*) onto the CCD camera (*CCD*). Images are captured by the VME computer and sent to a SUN workstation.

stepmotor on the filterwheel, the positions of which ("340 nm," "380 nm," or "dark") were controlled by an electronic controller and computer programs integrated into the imaging software. The software modifications as well as the filterwheel controller were custom made.

The fluorescent light emitted from the cells was first separated from the excitation light by a dichroic beam splitter at 395 nm mounted below the objective (Zeiss 63*, oil) and then passed a barrier filter at 500–530 nm. The fluorescence images were captured by a slow scan CCD camera (16 bits/pixel; Photometrics, CE 200, Tucson, Arizona) and read into the VME computer. The CCD readout frequency was 40 kHz. Rather than taking full frame images, we

usually read subarrays of the CCD array of ~100 × 150 pixels which contained the entire cell. Integration time varied between 500 and 3,000 ms according to dye loading conditions.

Background images were taken at 340 and 380 nm before the actual recording of calcium-dependent fluorescence. When the dye was loaded through the patch pipette, background images were taken before the cells were sealed. In the case in which the cells were loaded with fura-2/AM, an appropriate site of the experimental chamber where no cells were present was taken as background. In cases where Amiloride was added to the bath solution, the increased fluorescence levels caused by Amiloride were used as background.

Concentration values for intracellular calcium were estimated according to the standard ratioing algorithm described by Grynkiewicz, Poenie, and Tsien (1985). Calibration was performed in situ, i.e., pipette solutions with a very low Ca^{2+} (10 mM EGTA, nominally no Ca^{2+}), a known Ca^{2+} (105 nM, as determined by a Ca/Bapta mixture; Marks and Maxfield, 1991), and a high Ca^{2+} concentration (10 mM) were used to measure and calculate the corresponding fluorescence intensities and ratios, respectively. In the case of known Ca^{2+}, it was assumed that the cellular calcium control mechanisms did not markedly affect the calibration because a high Bapta concentration (10 mM) was used.

Calibration resulted in constants $R_{min} = 0.05$, $R_{max} = 1.6$, and an apparent $K_d^* = 1{,}117$ nM. Using the pipette calibration solutions with low and high Ca^{2+} at 380 nm, the ratio of the resulting fluorescence values was 8.4. Considering the ionic strength of 0.1 M of our pipette solutions, the resulting K_d of fura-2 with respect to calcium, i.e., $K_d = 1{,}117/8.4 = 133$ nM, was comparable to the value reported by Grynkiewicz et al. (1985). Calcium concentrations were then calculated according to (Grynkiewicz et al., 1985)

$$Ca^{2+} = K_d^* (R - R_{min})/(R_{max} - R).$$

The calibration measurements were repeatedly performed and the results were pooled. They are valid only under our particular experimental configuration of filters, objective, illumination, et cetera. We also performed calibration measurements in droplets of the above given solutions. The resulting calibration constants led, however, to considerably lower Ca^{2+} concentrations. We used the in-situ calibration because calibration and recording conditions were similar to each other.

The images were directly viewed during the experiments and then sent to a SUN sparc station I for subsequent processing and representation. The images shown below were photographed from the screen of the workstation.

RESULTS

Fig. 2 shows the spatial distribution of the calcium concentration in an olfactory receptor neuron held under voltage clamp conditions in the whole cell configuration of the patch clamp technique. The calcium concentration in the bath was 1 mM (solution R1). The spatial distribution of Ca_i^{2+} was clearly nonhomogenous, the concentration being higher in the dendritic knob (188 nM) than in the soma (51 nM). We repeated this experiment under identical conditions in five other cells and found in all cases a similar calcium gradient with increasing concentrations from the soma to the dendritic knob. The calcium values Ca_k^{2+} in the knob and Ca_s^{2+} in the soma (given as Ca_k^{2+}/Ca_s^{2+}, both in nM) were 80/15, 50/20, 35/12, 79/19, and 85/15. For the purposes of this paper it was convenient to indicate the increase of calcium concentration from soma to knob by a factor g defined as $g = Ca_k^{2+}/Ca_s^{2+}$. The g-factors for these five cells were 5.3, 2.5, 2.9, 4.2, and 5.6.

This inhomogenous distribution of the calcium concentration within the cells suggested a permeability of the plasma membrane for Ca^{2+} and a sink for Ca^{2+}, which lowered the calcium concentration in the soma with respect to other compartments of the cell. Common neuronal Ca^{2+} removal mechanisms are the Ca^{2+}-ATPase and the Ca/Na-transporter (Blaustein, 1988). Additionally, Ca_i^{2+} in the soma must be assumed to be influenced by EGTA and Ca-EGTA diffusing between pipette and cell (Neher and Augustine, 1992). To avoid this effect, we loaded 23 olfactory cells with the ester form of fura-2 (fura-2/AM) and observed Ca_i^{2+} under this condition. Fluorescence intensities in cells loaded with fura-2/AM were comparable to those measured in cells loaded through the patch pipette. Further, in the cells loaded with

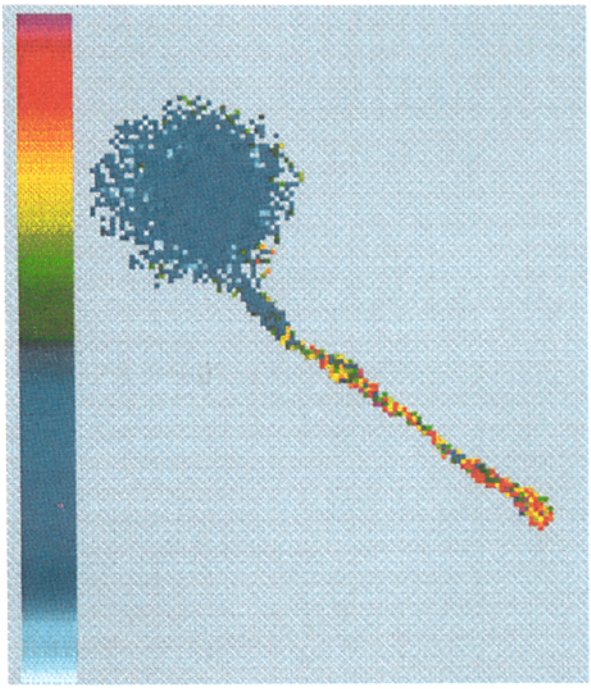

FIGURE 2. Fluorescence image of a patch clamped olfactory cell. The cell was clamped in the whole cell configuration at a membrane potential of −80 mV. Fura-2 entered the cell through the patch pipette. The calculated concentrations are pseudo color coded, whereby low, medium, and high concentrations are represented by colors ranging from blue over green to red. In this image, minimum and maximum concentrations are 0 and 180 nM, respectively. There is a gradient of Ca_i^{2+} from the soma to the dendritic knob.

fura-2/AM and in patch clamped cells that were supplied with ATP, the intracellular calcium concentrations were in the same range (Fig. 3), whereas in cells that were neither supplied with ATP through the pipette nor with glucose from the bath, Ca_i^{2+} assumed values of ~500 nM shortly after the establishment of the whole-cell configuration (Fig. 3). This indicated that ATP was required for holding Ca_i^{2+} at steady state concentrations of ~35 nM and also that the efflux of Ca_i^{2+} from the soma into the pipette could not prevent an increase in Ca_i^{2+} in the case in which neither glucose nor ATP were supplied.

Fig. 4 shows the spatial distributions of Ca_i^{2+} in a cell loaded with fura-2/AM (Ca_o^{2+} = 20 μM). In the cell shown on the left, the calcium concentration in the

dendritic knob as well as in the entire dendrite was obviously higher than in the soma ($g = 105/46 = 2.3$). 19 out of 23 observed cells showed a similar gradient of Ca_i^{2+}, whereas in four cells Ca_i^{2+} was spatially homogenously distributed. Fig. 5 gives the statistical distribution of calcium concentrations in soma and knob. In the soma, the concentrations were limited to values lower than 100 nM with a mean of 36 nM, whereas in the dendritic knob, concentrations were spread between 20 nM and 200

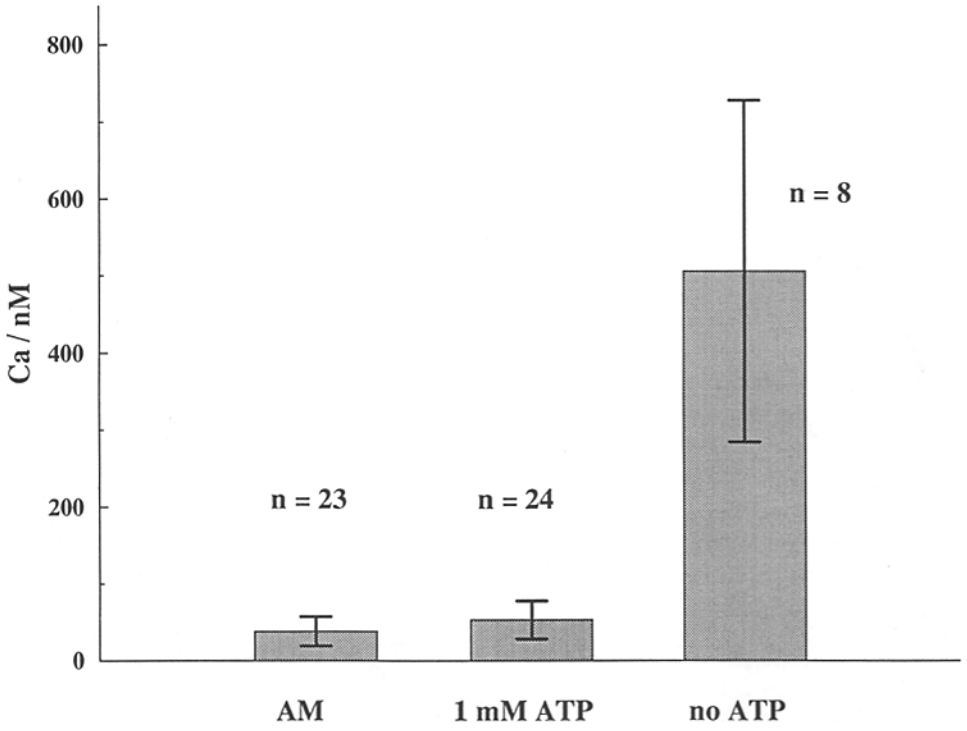

FIGURE 3. Calcium concentration in olfactory neurons under different experimental conditions. Mean values of Ca_i^{2+} are shown in cells which were loaded with fura-2/AM and had glucose in the bath solution (23 cells); which were held under patch clamp whole cell conditions with 1 mM ATP in the pipette solution (24 cells); and which were held under whole cell conditions without ATP in the pipette solution (8 cells). Cells to which either glucose (*AM*) or ATP (*ATP*) was supplied had low calcium concentrations (35–40 nM). In cells which were not supplied with glucose or ATP, Ca_i^{2+} was ~500 nM (no ATP).

nM with a mean of 87 nM. In the cells showing a gradient of Ca_i^{2+}, the mean calcium concentration in the soma was 49 nM, while it was 106 nM in the dendritic knob. The g-factors varied between 1.7 and 3.4. Factors higher than this, as observed under whole-cell conditions (see above), were never found. In all cells which showed a Ca_i^{2+} gradient, the calcium concentration in both the dendritic knob as well the soma increased when the bath concentration Ca_o^{2+} was increased from 20 μM to 5 mM.

With Ca_o^{2+} = 5 mM the mean concentration in the soma and the dendritic knob were 107 and 215 nM, respectively (g = 2).

In conclusion, the gradient of Ca_i^{2+} seen under whole-cell voltage clamp conditions was also present, though less pronounced, in most but not all of the cells which were loaded with fura-2/AM.

A standing gradient of Ca^{2+} within a cell requires a source, i.e., calcium influx into the cell, as well as a sink, i.e., calcium removal from the cell. Four ways have been described by which Ca^{2+} could enter olfactory cells: (*a*) an HVA Ca^{2+}-conductance (Trotier, 1986; Firestein and Werblin, 1987; Schild, 1989); (*b*) the Ca/Na-transporter driven in reversed mode (Schild and Bischofberger, 1991); (*c*) the cAMP-gated generator conductance, which can be blocked by Amiloride (Frings and Lindemann, 1988); and (*d*) IP_3-mediated conductance, which can be blocked by Ruthenium Red (Restrepo et al., 1990). Considering that the HVA Ca^{2+} conductance is not activated

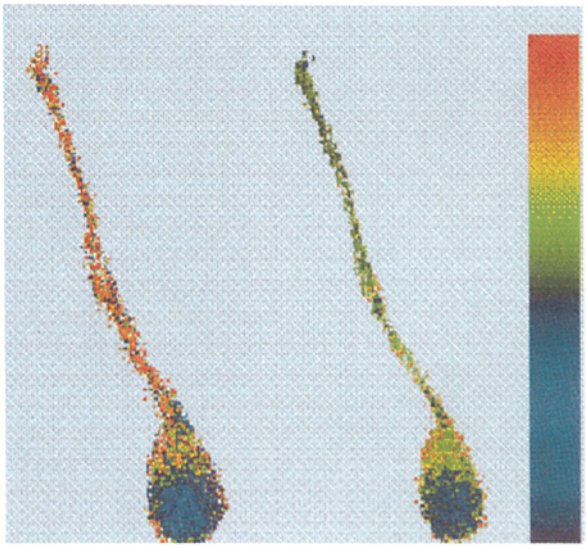

FIGURE 4. Fluorescence images of an olfactory cell loaded with fura-2/AM. Bath calcium concentration was 0.02 mM. The cell on the left side has a calcium concentration of ~105 nM in the whole dendrite and a lower concentration (46 nM) in the soma. The image on the right side shows the same cell after application of Amiloride. The calcium gradient is reduced, Ca_i^{2+} being 68 nM in the dendritic knob and 58 nM in the soma. Pseudo color coding is from 12 nM (*dark blue*) to 110 nM (*red*) in these images.

in the range of the membrane resting potential, and that, under physiological conditions, the Na/Ca-transporter is not driven in reversed mode at the resting potential, Ca^{2+} could possibly enter the cell through an Amiloride-sensitive or a Ruthenium Red-sensitive conductance. Alternatively, an as yet unknown conductance or possibly an artefactual leak conductance could underly the influx of Ca^{2+}. We tried to differentiate between these cases by adding Amiloride or Ruthenium Red to the bath.

In the cells which showed a gradient of Ca_i^{2+}, we exchanged the bath solutions with corresponding solutions to which Amiloride (50 μM) or Ruthenium Red (10 μM) was added. In 42% of the cells, Amiloride substantially reduced the gradient of Ca_i^{2+} while Ruthenium Red had no effect. The cell shown in Fig. 4 was one of the Amiloride-sensitive cells and on the right of the figure, the cell is shown 30 s after the application of Amiloride. Under control conditions (Fig. 4, left), the g-factor was g =

105/46 nM = 2.3, whereas it was g = 68/58 nM = 1.17 after Amiloride application. Apart from this immediate effect of Amiloride, it also led to a delayed and comparatively slow increase of the calculated values for Ca_i^{2+} both in soma and dendritic knob. Fig. 6 exemplifies both effects over time in a cell different from the one shown in Fig. 4. As discussed below, the delayed effect of Amiloride has to be interpreted with caution.

Ruthenium Red abolished the calcium gradients in 33% of the cells and no immediate reaction upon Amiloride was observed in these cells. Calcium concentrations before and after drug application were similar to those measured in Amiloride-sensitive cells. The reduction of the gradients brought about by the application of Ruthenium Red and Amiloride is summarized in Fig. 7. The mean g-factors before

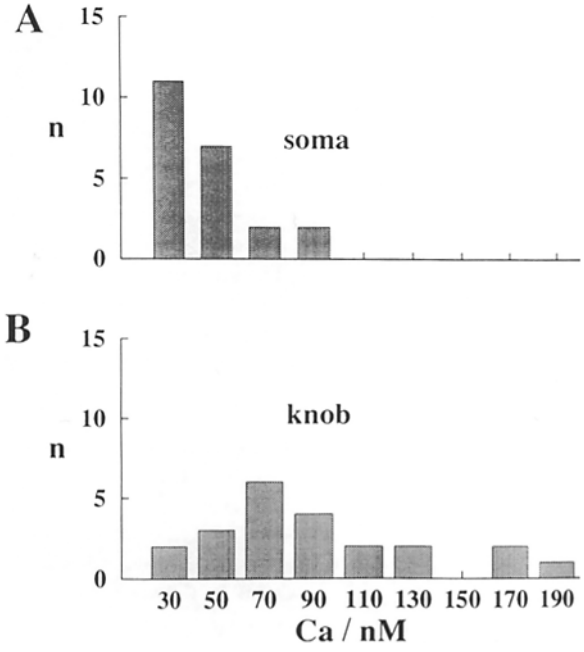

FIGURE 5. Distribution of Ca_i^{2+} in somata and dendritic knobs of olfactory cells. The number n of occurrence of the indicated calcium concentrations are shown. The single bars in both histograms go from 20 to 40 nM, from 40 to 60 nM, et cetera. and the mean concentration of every bar is indicated below the respective bar. The distribution of the calcium concentration in the soma (*A*) was highly asymetrical with a mean of 36 nM falling into the lowest histogram bar. Calcium concentrations in the dendritic knobs (*B*) were between 20 and 200 nM.

drug application were 2.22 ± 0.24 (Amiloride) and 2.08 ± 0.21 (Ruthenium Red), while they were reduced to 1.16 ± 0.04 (Amiloride) and 1.16 ± 0.14 (Ruthenium Red) after drug application.

These results indicated that an influx of calcium occurred through conductances that could be blocked either by Amiloride or by Ruthenium Red. However, in 25% of the cells neither drug affected the gradient.

DISCUSSION

We have used the calcium sensitive dye fura-2 (Grynkiewicz et al., 1985) as a pentapotassium salt and its membrane permeable form (acetoxymethylester, AM) to measure the calcium concentration in olfactory receptor neurons of the clawed frog

Xenopus laevis. Similar recordings in olfactory cells of the Channel catfish have been reported by Restrepo et al. (1990) and Restrepo and Boyle (1991). The resting concentrations in both species are in a comparable range (23 nM in the catfish and 36 nM in the soma of olfactory cells of *Xenopus*). However, due to the known difficulties to assign exact calcium concentrations to the measured fluorescence values (e.g., discussion in Grynkiewicz et al., 1985), the calculated calcium concentrations have to be regarded as estimates. Relative temporal and spatial changes in Ca_i^{2+} are thus, more significant than comparisons of absolute values among different experimental conditions.

We first recorded from cells that were loaded with the membrane impermeable fura-2 through the patch pipette, i.e., a seal (> 3 GΩ) was made between pipette and the cell's membrane, the patch broken by brief suction or negative voltage pulses,

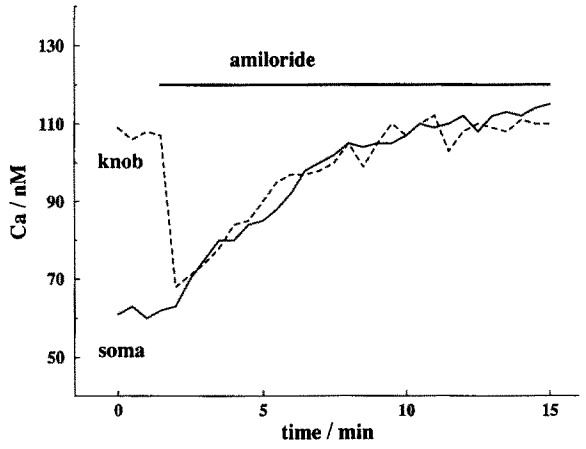

FIGURE 6. Effects of Amiloride upon the intracellular calcium concentration. The time courses of Ca_i^{2+} in the dendritic knob and the soma are plotted before and during application of Amiloride. Before drug application, steady state calcium levels in knob and soma were ~ 108 and 62 nM, respectively. Amiloride application is followed by a steep decrease of Ca_i^{2+} in the knob whereas Ca_i^{2+} in the soma is virtually not affected at this time. Over the next 10 min, Ca_i^{2+} both in the soma and the knob rises in a very similar way and is proportional to the function $f(t) = 1 - \exp(t/t_0)$ with $t_0 \sim 5$ min.

and fura-2 diffused from the pipette into the cell. In these cases, we always observed that the calcium concentration in the soma was lower than in the dendritic knob, and also slightly lower than in the somata of cells loaded with fura-2/AM. We have focused here on the comparison of calcium concentrations between dendritic knob and soma because in most cases, in particular when dendrites were very long (up to 120 μm), some parts of the dendrites were out of focus, so that it was usually impossible to measure the calcium concentrations over the entire length of the dendrite.

In all cases of observed gradients, calcium was highest in the dendritic knob and lowest in the soma. It can be assumed that calcium entered the cell primarily in its peripheral compartments and was removed primarily from the soma.

However, the whole-cell configuration of the patch clamp technique gave rise to an ambiguity since EGTA (3 mM in the pipette solution) must be considered to influence the calcium concentration in the cell. Even after a time at which diffusion of small molecules including EGTA between cell and patch pipette was equilibrated (Pusch and Neher, 1988), EGTA diffusing from the pipette to the cytosol must be assumed to be less saturated on the average than EGTA diffusing from the cytosol to the pipette. The diffusion of EGTA and EGTA-Ca between soma and pipette is thus a sink of free cytosolic calcium (Neher and Augustine, 1992).

To understand whether or not the observed gradients of calcium were mainly due to the described effect of EGTA or whether they were a characteristic feature of these cells, we loaded the cells with the ester form of fura-2. Under these conditions, only 25% of the cells had a homogenous spatial distribution of a low calcium concentration of ~35 nM. In these cells, Ca^{2+} presumably did not enter the cell at rest, at least not to a degree that could induce a detectable gradient of calcium.

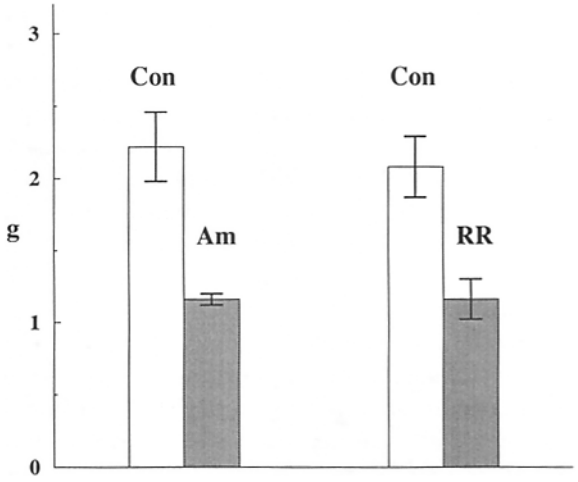

FIGURE 7. Blocking effects of Amiloride and Ruthenium Red upon intracellular calcium gradients. G-factors, i.e., the ratios of Ca_i^{2+} in the dendritic knob and the soma, are represented before (*Con*, control) and during application of the drugs Amiloride (*Am*) or Ruthenium Red (*RR*). In either case, the gradients measured under control conditions were almost abolished.

All other observed cells loaded with fura-2/AM showed higher calcium concentrations in the dendritic knob. It was not critical to decide whether or not there was a calcium gradient because the concentration in the knob was at least 1.7 times higher than in the soma, and the absolute difference of concentrations became larger when the calcium concentration in the bath was increased from 0.02 to 5 mM.

The olfactory neurons showed a diversity in how the gradient was affected by the drugs Ruthenium Red and Amiloride. Both drugs have been reported to affect olfactory generator conductances. Ruthenium Red blocks IP_3-mediated depolarizations in olfactory cells of the channel cat fish (Restrepo et al., 1990) and Amiloride blocks odor induced responses of the membrane potential as well as odor induced spiking activity in the frog (*rana esculenta;* Frings and Lindemann, 1988, 1990). In olfactory cells of *Xenopus,* both drugs had an effect and abolished the Ca^{2+} gradient in 75% of the cells. The reduction of the gradient was in all cases clear-cut from *g*-factors of ~2 to g-factors of ~1, so that it was in no case a problem to decide

whether or not a reduction had taken place (Fig. 7). Interestingly, no cell was affected by both drugs. It is beyond the scope of this paper to assess with statistical accuracy the frequencies of the cases (*a*) Ruthenium Red blocks the gradient; (*b*) Amiloride blocks the gradient; or (*c*) neither drug has an effect. A much larger sample of cells would be necessary for this purpose, and other techniques such as immunohistochemical binding studies might prove more promising in this respect.

The most plausible explanation for the observed effect of the drugs upon the calcium gradients is to assume two different conductances in the peripheral compartments of the cells that are permeable for calcium ions and that can be blocked either by Amiloride or by Ruthenium Red. Those cells that showed no change of the gradient upon drug application could either possess a third as yet unknown conductance permeable for calcium or, alternatively, there could have been an artefactual leakage of calcium into the cells.

Whether the cells that showed a standing calcium gradient were in fact at rest or stimulated by some unknown compound in the bath cannot be answered unambiguously. Usually, we apply odor stimuli at a concentration of 10 μM, and we have never observed odor responses in the nanomolar range. As we kept the bath as clean as possible, a contamination of the bath by known stimuli at micromolar concentrations is very unlikely. However, the action of an unknown stimulus cannot be completely ruled out.

An exact localization of the calcium source, i.e., dendritic knob and/or cilia, was impossible, because the cilia were usually (*a*) out of focus; (*b*) moving; and (*c*) had in any case too small a volume for recording sufficiently high fluorescence intensities. Our results did thus not allow distinguishing between calcium influx into cilia or calcium influx into the dendritic knob or both.

A conductance permeable to calcium inevitably would lead to a local increase of the calcium concentration. As an example, the volume of the dendritic knob is $\sim 4*10^{-15}$ l. A calcium current of 100 fA entering the knob means that $\sim 3 \cdot 10^5$ calcium ions enter the knob per second which would lead to an increase in calcium concentration of ~ 100 μM/s if all removal and buffering mechanisms as well as diffusion into other compartments are neglected. This simple example stresses the importance of removal, uptake, and buffering mechanisms but also the idea that even smaller calcium currents entering the dendritic knob could easily increase the local calcium concentration in the μM-range.

We limited ourselves in this study to the measurement of slow, steady state processes. Faster processes, such as the influence of odor stimulation upon intracellular calcium, should be investigated at a higher time resolution. Measurements of this type have been made on a different experimental setup and are reported elsewhere in preliminary form (Schild and Lischka, 1992).

Amiloride had two effects upon the observed fluorescence intensities. The delayed effect cannot be interpreted quantitatively, because Amiloride is fluorescent when illuminated at 340 nm or 380 nm, and it is taken up by cells (Briggman, Graves, Spicer, and Cragoe, 1983). The ratio R used to estimate the calcium concentrations is therefore contaminated by the fluorescence intensities A340 and A380 of Amiloride

at the wavelengths 340 and 380 nm,

$$R = \frac{\text{F340} + \text{A340} - \text{B340}}{\text{F380} + \text{A380} - \text{B380}},$$

with background fluorescences B340 and B380 that include the Amiloride dependent fluorescences. The Ca-dependent fluorescence intensities F340 and F380 are thus superimposed with A340 and A380. In control measurements, in which we applied only Amiloride and no fura-2, A340 and A380 increased over 10 min to about steady state values. A340 was virtually negligible as compared to A380 which corresponds well to the excitation spectrum of Amiloride (Briggman et al., 1983). The steady state value A380 was ~8% of the fluorescence intensity we observed when the cell were additionally loaded with fura-2/AM. At the beginning of the Amiloride application, both fluorescences, A340 and A380, were negligible so that the immediate effect of Amiloride upon the calcium gradient can be regarded as reliable and not affected by the uptake of Amiloride by the cells. Over the following minutes the function A380(t) increased and thereby introduced an artefactual decrease of the ratio R.

In conclusion, Amiloride caused a block of a calcium source in the dendritic knob and then led to an increase of Ca_i^{2+}. Due to the Amiloride-dependent fluorescence A380, the calculated increase in calcium was presumably lower than the increase in the real calcium concentration.

From the results and discussion of the observed calcium gradients, it is obvious that the calcium removal mechanisms, their localization, and their impact on transduction need further investigation. The comparison of patch clamped cells to which ATP was or was not supplied have revealed that an ATP dependent mechanism certainly contributes to maintaining low calcium concentration in olfactory cells of *Xenopus laevis* (Fig. 3). The Ca-ATPase seems to be the most probable candidate. Ca_i^{2+} in patch clamped cells with ATP supplied to the cytosol was ~35 nM and very similar to Ca_i^{2+} in cells loaded with fura-2/AM. On the other hand, when ATP was omitted from the patch pipette, Ca_i^{2+} was ~500 nM and stayed at this level in every single cell. This appears to indicate the existence of a second calcium removal mechanism which operates in this range of concentrations. Though there is preliminary evidence for the existence of the Na/Ca exchanger in these cells (Schild and Bischofberger, 1991) and though the K_d of the neuronal Na/Ca exchanger is ~500 nM (Blaustein, 1988), the characterization and localization of the Na/Ca-transporter in olfactory cells remain to be investigated.

Original version received 26 March 1993 and accepted version received 24 May 1993.

REFERENCES

Boekhoff, I., E. Tareilus, J. Strotmann, and H. Breer. 1990. Rapid activation of alternative second messenger pathways in olfactory cilia from rats by different odorants. *Embo Journal.* 9:2453–2458.

Blaustein, M. P. 1988. Calcium transport and buffering in neurons. *Trends in Neurosciences.* 11:438–443.

Breer, H., I. Boekhoff, and E. Tareilus. 1990. Rapid kinetics of second messenger formation in olfactory transduction. *Nature.* 345:65–68.

Briggman, J. V., J. S. Graves, S. S. Spicer, and E. J. Cragoe, Jr. 1983. The intracellular localization of amiloride in frog skin. *Histochemical Journal.* 15:239–255.

Buck, L., and R. Axel. 1991. A noval multigene family may encode odorant receptors: a molecular basis for odor recognition. *Cell.* 65:175–187.

Dhallan, R. S., K.-W. Yau, K. A. Schrader, and R. R. Reed. 1990. Primary structure and functional expression of a cyclic nucleotide-activated channel from olfactory neurons. *Nature.* 347:184–187.

Dionne, V. E. 1992. Chemosensory responses in isolated olfactory receptor neurons from *Necturus maculosus*. *Journal of General Physiology.* 99:415–433.

Firestein, S., and F. S. Werblin. 1987. Gated currents in isolated olfactory receptor neurons of the larval tiger salamander. *Proceedings of the National Academy of Sciences, USA.* 84:6292–6296.

Firestein, S., and F. S. Werblin. 1989. Odor-induced membrane currents in vertebrate-olfactory receptor neurons. *Science.* 244:79–82.

Firestein, S., G. M. Shepherd, and F. S. Werblin. 1990. Time course of the membrane current underlying sensory transduction in salamander olfactory receptor neurones. *Journal of Physiology.* 430:135–158.

Frings, S., and B. Lindemann. 1988. Odorant response of isolated olfactory receptor cells is blocked by Amiloride. *Journal of Membrane Biology.* 105:233–243.

Frings, S., and B. Lindemann. 1990. Response of olfactory receptor cells, isolated and in situ, to low concentrations of odorants. *In* Chemosensory Information Processing. D. Schild, editor. Springer Verlag, Berlin. 233–243.

Frings, S., J. W. Lynch, and B. Lindemann. 1992. Properties of cyclic nucleotide-gated channels mediating olfactory transduction. *Journal of General Physiology.* 100:45–67.

Grynkiewicz, G., M. Poenie, and R. Y. Tsien. 1985. A new generation of Ca^{2+} indicators with greatly improved fluorescence properties. *Journal of Biological Chemistry.* 260:3440–3450.

Hamill, O. P., A. Marty, E. Neher, B. Sakmannn, and F. J. Sigworth. 1981. Improved patch-clamp techniques for high-resolution current recording from cells and cell-free membrane patches. *Pflügers Archiv.* 391:85–100.

Jones, D. T., and R. R. Reed. 1989. G_{olf}: an olfactory neuron specific-G protein involved in odorant signal transduction. *Science.* 244:790–795.

Kleene, S. J., and R. C. Gesteland. 1991. Calcium-activated chloride conductance in frog olfactory cilia. *Journal of Neuroscience.* 11:3624–3629.

Kurahashi, T. 1989. Activation by odorants of cation-selective conductance in the olfactory receptor cell isolated from the newt. *Journal of Physiology (Lond.).* 419:177–192.

Kurahashi, T. 1990. The response induced by intracellular cyclic AMP in isolated olfactory receptor cells of the newt. *Journal of Physiology (Lond.).* 430:355–371.

Kurahashi, T., and T. Shibuya. 1989. Membrane response and permeability changes to odorants in the solitary receptory cells of newt. *Zoological Science.* 6:19–30.

Kurahashi, T., and T. Shibuya. 1990. Ca^{2+}-dependent adaptive properties in the solitary olfactory receptor cell of the newt. *Brain Research.* 515:261–268.

Lischka, F. W., and D. Schild. 1993. Effects of nitric oxide upon olfactory receptor neurons in Xenopus laevis. *NeuroReport.* 4:582–584.

Lynch, J. W., and B. Lindemann. 1992. Divalent cations decrease sensitivity of cAMP-gated channels to cAMP in rat olfactory receptor cells. *Chemical Senses.* 17:860.

Marks, P. W., and F. R. Maxfield. 1991. Preparation of solutions with free calcium concentrations in the nanomolar range using 1,2-bis(o-aminophenoxy)ethane-*N,N,N′, N′*-tetraacetic acid. *Analytical Biochemistry.* 193:61–71.

Nakamura, T., and G. H. Gold. 1987. A cyclic nucleotide-gated conductance in olfactory receptor cilia. *Nature.* 325:442–444.

Neher, E., and G. J. Augustine. 1992. Calcium gradients and buffers in bovine chromaffin cells. *Journal of Physiology.* 450:273–301.

Pace, U., E. Hanski, Y. Salomon, and D. Lancet. 1985. Odorant-sensitive adenylate cyclase may mediate olfactory reception. *Nature.* 316:255–258.

Pusch, M., and E. Neher. 1988. Rates of diffusional exchanges between small cells and a measuring patch pipette. *Pflügers Archiv.* 411:204–211.

Restrepo, D., and A. G. Boyle. 1991. Stimulation of olfactory receptors alters regulation of $[Ca_i]$ in olfactory neurons of the catfish (*Ictalurus punctatus*). *Journal of Membrane Biology.* 120:223–232.

Restrepo, D., and J. H. Teeter. 1990. Olfactory neurons exhibit heterogeneity in depolarization-induced calcium change. *American Journal of Physiology.* 258:C1051–C1061.

Restrepo, D., T. Miyamoto, B. C. Bryant, and J. H. Teeter. 1990. Odor stimuli trigger influx of calcium into olfactory neurons of the channel catfish. *Science.* 249:1166–1168.

Schild, D. 1989. Whole-cell currents in olfactory receptor cells of *Xenopus laevis*. *Experimental Brain Research.* 78:223–232.

Schild, D., and J. Bischofberger. 1991. Ca^{2+} modulates an unspecific cation conductance in olfactory cilia of *Xenopus laevis*. *Experimental Brain Research.* 84:187–194.

Schild, D., and F. W. Lischka. 1992. High time resolution recordings of stimulus dependent calcium increase in *Xenopus* olfactory neurones measured with a laser scanning microscope. *Chemical Senses.* 17:879*a* (Abstr.).

Sklar, P. B., R. R. H. Anholt, and S. H. Snyder. 1986. The odorant-sensitive adenylate cyclase of olfactory receptor cells. *Journal of Biological Chemistry.* 261:15538–15543.

Trotier, D. 1986. A patch-clamp analysis of membrane currents in salamander olfactory receptor cells. *Pflügers Archiv.* 407:589–595.

Zufall, F., G. M. Shepherd, and S. Firestein. 1991. Inhibition of the olfactory cyclic nucleotide gated ion channel by intracellular calcium. *Proceedings of the Royal Society of London, B. Biological Sciences.* 246:225–230.